Pharmacological Reports 71 (2019) 535–544

Contents lists available at ScienceDirect

Pharmacological Reports

journal homepage: www.elsevier.com/locate/pharep

Original article

Transcriptome-based identification of lovastatin as a breast cancer stem cell-targeting drug

Luz X. Vásquez-Bochm[a,b], Mireya Velázquez-Paniagua[a,c], Sandra S. Castro-Vázquez[a], Sandra L. Guerrero-Rodríguez[a], Abimael Mondragon-Peralta[a], Marisol De La Fuente-Granada[d], Sonia M. Pérez-Tapia[e], Aliesha González-Arenas[d], Marco A. Velasco-Velázquez[a,f,*]

[a] Department of Pharmacology, School of Medicine, National Autonomous University of Mexico (Universidad Nacional Autónoma de México; UNAM), Mexico City, Mexico
[b] Graduate Program in Chemical Sciences, UNAM, Mexico City, Mexico
[c] Department of Physiology, School of Medicine, UNAM, Mexico City, Mexico
[d] Department of Genomic Medicine and Environmental Toxicology, Institute of Biomedical Research (IIB), UNAM, Mexico City, Mexico
[e] Unit for Development and Research in Bioprocesses (UDIBI), National School of Biological Sciences, National Polytechnic Institute, Mexico City, Mexico
[f] Unit for Research in Translational Biomedicine, Research Division, School of Medicine, UNAM, Mexico City, Mexico

ARTICLE INFO

Article history:
Received 7 August 2018
Received in revised form 27 January 2019
Accepted 15 February 2019
Available online 16 February 2019

Keywords:
Breast cancer stem cells
Drug repurposing
Lovastatin
HMGCR inhibitor

ABSTRACT

Background: Breast cancer is a neoplastic disease with high morbidity and mortality in women worldwide. Breast cancer stem cells (CSCs) have a significant function in tumor growth, recurrence, and therapeutic resistance. Thus, CSCs have been pointed as targets of new therapies for breast cancer. Herein, we aimed to repurpose certain drugs as breast CSC-targeting agents.

Methods: We compared a consensus breast CSC signature with the transcriptomic changes that were induced by over 1300 bioactive compounds using Connectivity Map. The effects of the selected drugs on *SOX2* promoter transactivation, SOX2 expression, viability, clonogenicity, and ALDH activity in breast cancer cells were analyzed by luciferase assay, western blot, MTT assay, mammosphere formation assay, and ALDEFLUOR® test, respectively. Gene Set Enrichment Analysis (GSEA) was performed using the gene expression data from mammary tumors of mice that were treated with lovastatin.

Results: Five drugs (fasudil, pivmecillinam, ursolic acid, 16,16-dimethylprostaglandin E2, and lovastatin) induced signatures that correlated negatively with the query CSC signature. *In vitro*, lovastatin inhibited *SOX2* promoter transactivation, and reduced the efficiency of mammosphere formation and the percentage of $ALDH^+$ cells. Mevalonate mitigated the effects of lovastatin, suggesting that the targeting of CSCs by lovastatin was mediated by the inhibition of its reported target, 3-hydroxy-3-methyl-glutaryl-coenzyme A reductase (HMGCR). By GSEA, lovastatin down-regulated genes that are involved in stemness and invasiveness in mammary tumors, corroborating our *in vitro* findings.

Conclusion: Lovastatin is a breast CSC-targeting drug. The inhibition of HMGCR might develop new adjuvant therapeutic strategies for breast tumors.

Introduction

Breast cancer (BC) has a high incidence and causes significant mortality in women worldwide [1]. It is estimated that approximately 3.2 million new cases of BC will develop annually by 2050 [2]. Despite the implementation of new therapies and treatments, approximately one-third of BC patients die due to tumor resistance, recurrence, and metastasis [3].

The cancer stem cell (CSC) hypothesis proposes that a subpopulation at the top of the tumor cell hierarchy contributes to tumor heterogeneity and is uniquely able to seed new tumors. Breast cancer stem cells (BCSCs) can self-renew, express signaling

* Corresponding author.
E-mail address: marcovelasco@unam.mx (M.A. Velasco-Velázquez).

https://doi.org/10.1016/j.pharep.2019.02.011
1734-1140/

proteins and transcription factors that promote pluripotency, generate non-stem tumor cells, and initiate tumors when implanted into immunocompromised mice [4,5].

BCSCs play key roles in the therapeutic resistance, recurrence, and progression of human breast tumors [6,7]. BCSCs display resistance to cytotoxic drugs [8], hyperactivation of signaling pathways that control stemness [9], and heightened DNA repair [10]. Further, breast cancer cells that disseminate to bone marrow and metastasis-initiating cells [9,11] have a stem phenotype, indicating that the CSC pool drives metastasis. Thus, CSCs are targets for new therapies in BC [12,13].

Drug repurposing is the identification of new therapeutic indications for approved drugs [14]. This strategy has several advantages, including a lower risk of toxic effects, accelerated clinical validation, and the ability to patent its new use [15]. There are many approaches for detecting unrecognized or non-explicit connections between drugs, targets, and diseases, including computational modeling, studying the mechanism of action-based methods, genetic profiling, and translational bioinformatics [16].

Transcriptional profiling studies identify gene sets that are differentially expressed in diseases or cells that have been exposed to drugs [17–19]. The comparison of a disease-induced gene signature against the expression profiles that are generated by drug exposure can reveal new connections between drugs and the disease. Theoretically, the drugs that induce transcriptional changes that are opposite to those in the disease could revert the phenotype [20]. Thus, several databases and user interfaces have been developed to translate genomewide transcriptional analyses into drug discovery [21–23].

Connectivity Map (CMap) [24] is a public database that contains genomewide expression profiles of human cancer cell lines that have been treated with bioactive compounds. These profiles can be compared with gene sets of interest by a matching algorithm, based on Kolmogorov-Smirnov statistical analysis. CMap has been useful for drug repurposing, lead discovery, mechanism of action analyses, and systems biology [25]. For example, it has been used to identify new activities of drugs in various neoplastic [26,27] and non-cancerous diseases [28].

To repurpose drugs that target BCSCs, we used a consensus gene signature that defines BCSCs to query CMap. The candidates that we identified were evaluated *in vitro* in triple-negative breast cancer cells. We found that the drug lovastatin reduced the CSC pool and that this effect was attributed to the inhibition of 3-hydroxy-3-methyl-glutaryl-coenzyme A reductase (HMGCR). By bioinformatic analysis of an independent dataset, mammary cancer cells from lovastatin-treated mice downregulated genes that control stemness and invasiveness, corroborating our *in vitro* findings. Our results agree with previously identified effects of statins [29–31] and support the repurposing of lovastatin as a drug with efficacy against BCSCs.

Materials and methods

Chemical transcriptomics

We used build 02 of the CMap database [24]. As a query signature, we selected a reported consensus BCSC signature [12] that comprised 39 genes (25 upregulated and 14 downregulated) and was generated from 3 biologically validated signatures, comparing: i) paclitaxel- *versus* salinomycin-treated HMLER breast cancer cells [12]; ii) primary human mammary epithelial cells that were cultured under conditions that favor mammary epithelial stem cell expansion *versus* cells that were cultured under conditions that favor differentiation [32]; and iii) $CD44^+$ normal and neoplastic human mammary epithelial populations *versus* $CD24^+$ cells [33].

Candidate drugs were selected from the CMap results, based on: a) significant negative association with the query signature ($p < 0.5$); b) a mean score < -0.5; c) specificity value < 0.1; and d) percentage non-null $\geq$ 75%. The global transcriptional responses that were induced by the candidate drugs were compared using Mode of Action by NeTwoRk Analysis (MANTRA) [21] with a computed distance threshold of 0.7.

Compounds

Fasudil hydrochloride (HA-1077), pivmecillinam (SML0817), ursolic acid (89797), 16,16-dimethyl-prostaglandin E2 (PGE2) (D2250000), and lovastatin (PHR1285) were purchased from Sigma-Aldrich. The stock solutions were prepared in DMSO and stored at −70 °C under light-protected conditions until use. (±)-Mevalonolactone (Sigma-Aldrich M4667) solutions were prepared in water. The structural similarity of the candidate drugs was analyzed by generating fingerprints by circular and MACCS methods and comparing them using the Tanimoto coefficient, with the KNIME program in the CDK module.

Cell lines and culture

The triple-negative cell lines MDA-MB-231 and Hs578T were obtained from ATCC. The cells were grown in RPMI-1640 (MDA-MB-231) or DMEM (Hs578T) (Gibco) that was supplemented with 10% fetal bovine serum (FBS), at 5% CO_2 atmosphere. We used cell cultures from passage 6 to 16.

Luciferase assay

MDA-MB-231 cells were cotransfected with pGL3-*SOX2*-luc or pGL3-*OCT4*-luc plasmid [34] (generously donated by Dr. Richard Pestell, Baruch S. Blumberg Institute, PA, USA) and pNEG-PG04 using lipofectamine 3000 (Invitrogen) per the manufacturer's guidelines. Sublines that stably expressed the reporter constructions were selected and maintained in complete medium plus 0.5 μg/ml puromycin. Cells were incubated with drugs for 24 h; then, the medium was removed, and the cells were incubated with lysis buffer (1% Triton X-100, 1 mM DTT in GME buffer) for 10 min at room temperature with shaking. Homogenates were mixed with 3 volumes of assay buffer (17 mM K_2PO_4, 1 mM DTT, and 2 mM ATP in GME buffer). Luminescence was quantified immediately after the addition of luciferin (GOLDBIO) on a GloMax® 20/20 luminometer (Promega). The fraction of viable cells at each concentration of drug was quantified in the same experiment and used for normalization.

Cell viability

5,000 MDA-MB-231 or 3,000 Hs578T cells were seeded in 96-well microplates and exposed to drugs for 24 h. The effect of the drugs on cell viability was estimated by MTT [3-(4,5-dimethylthiazol-2-yl)-2,5-diphenyltetrazolium bromide] assay. Reduced tetrazolium salt was measured spectrophotometrically at 570 nm (Epoch, BioTeK). Two to three independent experiments, each with six technical replicates, were performed (see figure legends for details).

Mammosphere formation assay

Sphere formation assay was performed as reported [32]. Briefly, 100 viable cells/well were plated in 96-well ultra-low attachment plates (Corning Costar) with MammoCult medium and growth factors (StemCell Technologies). The spheres were quantified on Day 7 in micrographs (Eclipse Ti-U microscopy, Nikon) and analyzed with NIS-Elements Imaging Software 4.13 (Nikon). Each

independent experiment was performed in octuplicate. In some experiments, the drug was present throughout the 7-d incubation, whereas in others, the cells were pretreated for 24 h and cultured in drug-free medium (see figure legends for details). The results are presented as mammosphere-forming efficiency (MFE%), which was calculated with the following equation: MFE%= (number of mammospheres per well) / (number of cells seeded per well) x 100.

ALDH staining

Treated cells were analyzed with the ALDEFLUOR® assay kit (StemCELL Technologies) per the manufacturer's guidelines. Briefly, cells were harvested with 0.05% trypsin-EDTA (Gibco), washed, counted, and suspended in ALDEFLUOR® buffer (2.5×10^6 cells/mL). ALDH substrate was added to the sample, which was then divided immediately into 2, to one half of which 7 μL of the ALDH inhibitor DEAB was added. Both samples were incubated for 45 min at 37 °C before being analyzed on an Attune-NxT cytometer (Life Technologies). Data were analyzed in FlowJo 8.7 (Tree Star Inc.) using DEAB-treated controls to establish the negative fluorescence signal.

Table 1
Potential drugs targeting the BCSC phenotype.

Compound	P	Mean cMap score	Specificity
Fasudil	0.02382	−0.71	0
Spiperone	0.00592	−0.677	0.0088
Pivmecillinam	0.00438	−0.606	0.0111
Ursolic acid	0.00203	−0.601	0.0073
16,16-dimethylprostaglandin E2	0.00877	−0.572	0.0138
Lovastatin	0.0118	−0.527	0.0155

Western blot

Treated cells were lysed in RIPA buffer (50 mM Tris−HCl, 0.1% SDS, 150 mM NaCl) supplemented with protease inhibitors (5 μg/mL leupeptin, 1 μg/mL pepstatin, 2 μg/mL aprotinin). Protein

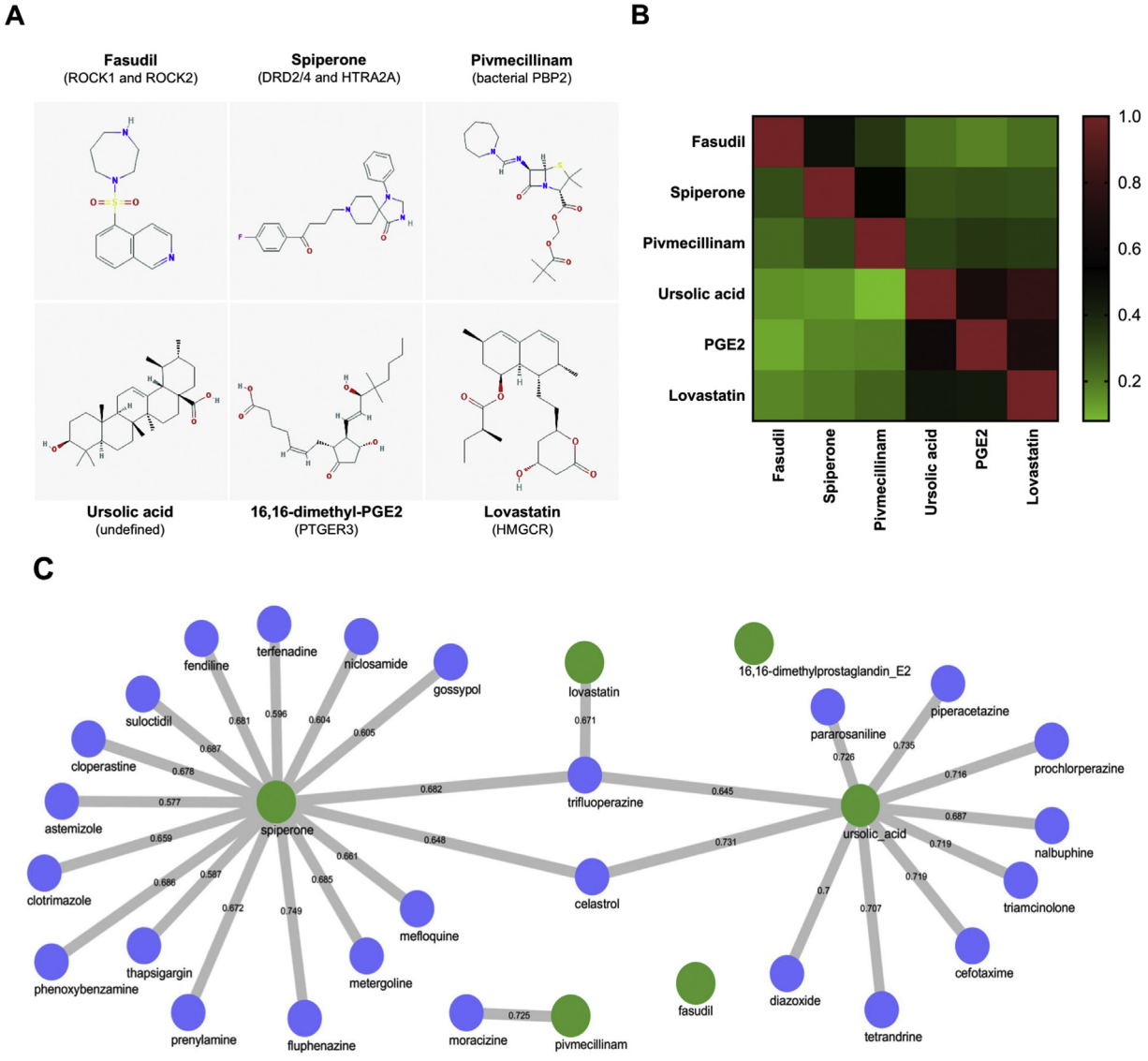

Fig. 1. Comparison of candidate drugs. A) Structure and reported targets of the six drugs selected in CMap. B) Chemical similarity evaluation by Tanimoto coefficient. Upper half of the matrix corresponds to the analysis based on fingerprint generation by MACCS, whereas the lower part shows the comparison using fingerprint generation by circular method. C) Comparison of global transcriptional changes induced by the candidate drugs (green circles). Drugs with significant associations are shown as blue circles. (For interpretation of the references to colour in this figure legend, the reader is referred to the web version of this article).

concentrations in the lysates were determined using the Pierce BCA Protein Assay Kit (Thermo Fisher Scientific). Samples that contained 30 μg of total protein were separated by SDS-PAGE and electroblotted onto PVDF membranes. After being blocked, the membranes were incubated with anti-SOX2 (Abcam ab97959; 1:1000), followed by a HRP-conjugated goat anti-rabbit secondary antibody (Santa Cruz Biotechnology sc-2004). The same membranes were stripped and reprobed with anti-α-tubulin (Santa Cruz Biotechnology sc-398103; 1:500), followed by a HRP-conjugated goat anti-mouse antibody (Abcam ab6789). Protein bands were detected using SuperSignal West Femto Maximum Sensitivity Substrate Pierce ECL Western Blotting Substrate (Thermo Fisher Scientific). Band intensities were measured in Image J [35] and data were normalized against vehicle (DMSO).

Enrichment analysis

Microarray data on 5 mouse mammary tumors that were treated with lovastatin and 5 controls were obtained from the Gene Expression Omnibus dataset GSE42787 [36]. Data were normalized in R studio (v1.1.383) using robust multi-array average normalization. Gene Set Enrichment Analysis (GSEA) [37] was performed using GSEA (v2.2.3). The following molecular signatures were used in the analysis: i) the Consensus Stemness Ranking (CSR) signature, [38]; ii) the oncogenic signature in mouse and human mammary stem cells [39]; iii) a hallmark gene set of the epithelial-to-mesenchymal transition (EMT) [40]; and iv) a signature from invasive ductal carcinomas [41]. Enrichment analysis for transcription factor targets was performed by feeding the top 250 differentially expressed genes into the ChiP-X Enrichment Analysis (ChEA) tool [42].

Statistical analysis

IC_{50} values were calculated by nonlinear regression. Unless otherwise noticed, statistical significance was determined by one-way ANOVA, followed by Dunnett's multiple comparisons test against the vehicle control. Graphs were constructed and statistical analyses were performed in Prism (GraphPad).

Results

In silico *prediction of drugs targeting BCSCs*

Using a BCSC gene expression signature [12], we ranked the 1309 compounds in the CMap platform. Based on the selection criteria (see "Materials and methods"), we identified several drugs that induced gene expression signatures that correlated negatively with those of BCSCs and thus represented potential therapeutic candidates (Table 1). The drugs were structurally distinct, had diverse canonical targets, and induced dissimilar global transcriptional signatures (Fig. 1). Of these candidates, we examined fasudil, pivmecillinam, ursolic acid, 16,16-dimethylprostaglandin E2 (PGE2), and lovastatin with regard to their activity in breast cancer cell cultures.

Lovastatin and fasudil reduce SOX2 promoter transactivation

SOX2 and OCT4 are essential regulators of cellular self-renewal and the maintenance of pluripotency in CSCs [43,44], and reporter constructs that harbor portions of their promoters have been used to monitor stemness in breast cancer cells [34,45]. In a primary screen, we measured the effects of the selected drugs on the transactivation of the *SOX2* and *OCT4* promoters at the concentration employed in CMap development (10 μM). Fasudil and lovastatin reduced *SOX2* promoter transactivation by 60% and 95%, respectively (Fig. 2A). Conversely none of the drugs had a significant effect on transactivation of the *OCT4* promoter (Fig. 2B). Based on these results, we focused on fasudil and lovastatin in subsequent analyses.

Lovastatin but not fasudil impairs clonogenicity

Using fasudil and lovastatin, we generated concentration-response curves to analyze their: i) cytotoxic effects in 2D cultures, ii) effects on mammosphere formation efficiency, and iii) impact on *SOX2* promoter transactivation at various concentrations. Lovastatin reduced the viability of MDA-MB-231 to 56% of that of the control at the highest concentration. In contrast, fasudil had a modest effect on cell viability (Fig. 3A). Lovastatin but not fasudil decreased the number of mammospheres (IC_{50} = 2.2 μM; Fig. 3B). Finally, both drugs impaired *SOX2* promoter transactivation (Fig. 3C), supporting the findings in the primary screen and indicating that lovastatin is more potent. Based on the effects of lovastatin on clonogenicity and *SOX2* promoter transactivation, we subjected it to additional analysis.

Short-term exposure of breast cancer cells to lovastatin irreversibly affects the CSC pool

Aldehyde dehydrogenase (ALDH) activity has been used extensively to quantify the CSC population in triple-negative

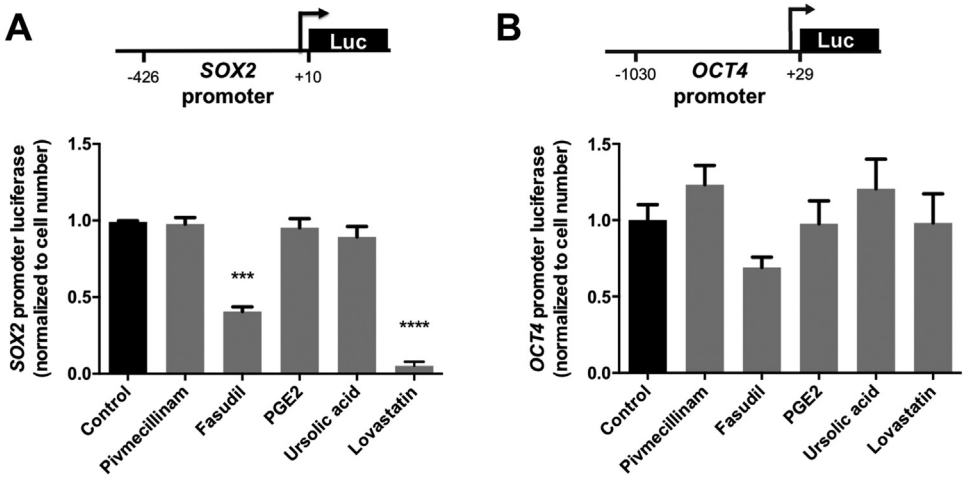

Fig. 2. Effects of the selected drugs on transactivation of the *SOX2* (A) and *OCT4* (B) promoters. Schemes above graphs show the size of the promoters in the constructs. Transactivation was measured by luciferase reporter assay. Values are mean ± SEM from 4 independent experiments; $p < 0.05$ (*), < 0.01 (**), < 0.001 (***), < 0.0001 (****).

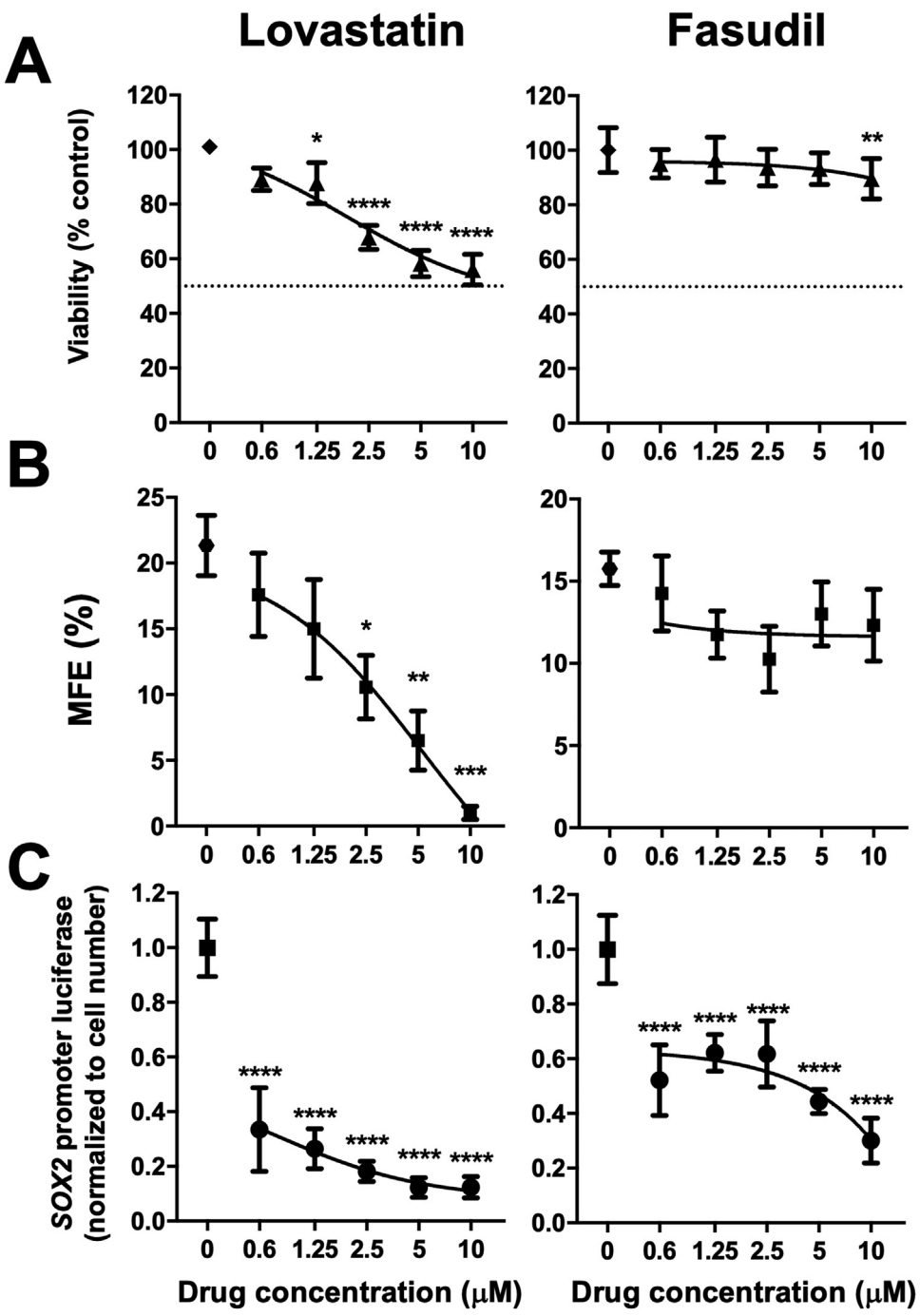

Fig. 3. Activity of presumed BCSC-targeting drugs. Effects of lovastatin or fasudil on MDA-MB-231 cell viability (A) and mammosphere-initiating capacity (B). The effects of the drugs on *SOX2* promoter transactivation were corroborated in dose-response curves (C). Graphs show mean ± SEM of a compilation of 3 independent experiments; $p <$ 0.05 (*), < 0.01 (**), < 0.001 (***), < 0.0001 (****) against the vehicle control.

breast cancer cells [46–48]. Lovastatin significantly reduced the ALDH$^+$ fraction in a concentration-dependent manner in MDA-MB-231 cells (Fig. 4B–C) and Hs578T cells (Fig. 4D and Suppl. Fig. 1B). The effects correlated with reductions in SOX2 protein expression in both cell lines (Fig. 4E). Together, these results supported the hypothesis that lovastatin decreases the CSC pool.

To confirm the CSC-targeting effects of lovastatin, we followed the strategy reported by Gupta and collaborators [12]. Cells were pre-incubated with lovastatin, collected and cultured to evaluate their mammosphere formation capacity under drug-free conditions (Fig. 4A). Pre-incubation significantly lowered the number of mammospheres in the two studied cell lines (Fig. 4F, G), supporting that lovastatin irreversibly reduces the CSC pool.

Effects of lovastatin on CSC are mediated by HMGCR inhibition

To determine whether the effects of lovastatin are mediated by its canonical target, we treated cells simultaneously with lovastatin and/or mevalonate, the latter of which is generated by HMGCR [49]. Mevalonate reverted the lovastatin-induced

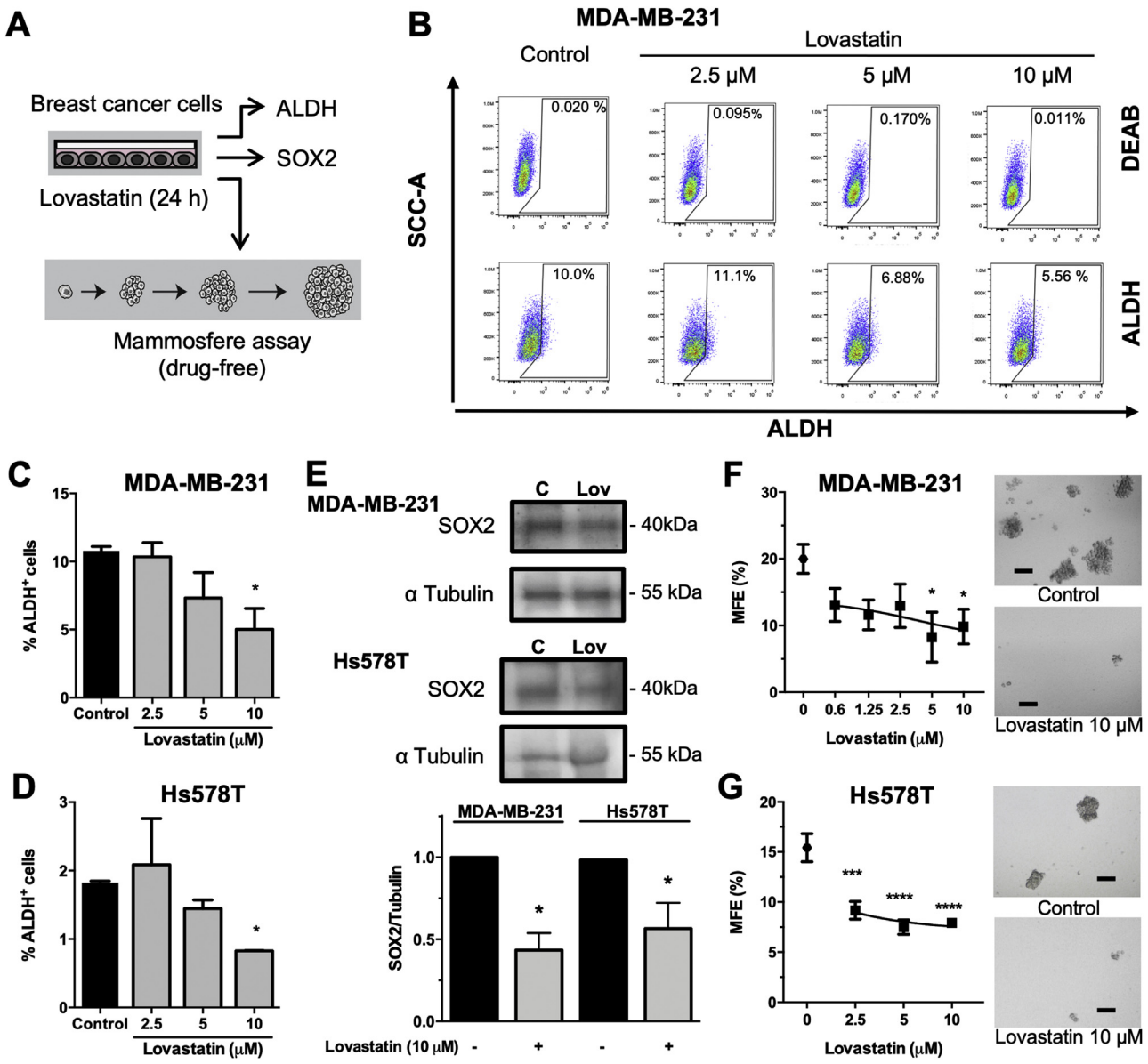

Fig. 4. Effects of lovastatin on the breast cancer stem cell pool. A) Experimental strategy for analyzing stemness after short exposure of breast cancer cells to lovastatin. B) Representative dot plots quantifying the ALDH$^+$ fraction in lovastatin-treated MDA-MB-231 cells. C, D) Analysis of ALDH$^+$ cells in MDA-MB-231 (C) and Hs578T (D) cells. Graphs show mean ± SEM from 5 (C) or 2 (D) independent experiments. E) Representative western blot evaluating the expression of SOX2 and the corresponding analysis of the SOX2/α-tubulin ratio from 3 independent experiments. Statistical significance was determined by Student's *t*-test. F, G) Viable MDA-MB-231 (F) or Hs578T (G) cells that had been exposed to lovastatin for 24 h were seeded to test their capacity to grow mammospheres in drug-free medium. Graphs show the mean number of mammospheres ± SEM from 4 independent experiments (F) or from a representative experiment performed in octuplicate (G). Representative pictures are shown; bar = 100 μm; $p <$ 0.05 (*), < 0.01 (**), < 0.001 (***), < 0.0001 (****).

decrease in the fraction of ALDH$^+$ cells (Fig. 5A) and mammosphere formation (Fig. 5B). Mevalonate also partially restored *SOX2* promoter transactivation, which was completely inhibited by lovastatin (Fig. 5C), and SOX2 protein expression (Fig. 5F). Notably, mevalonate alone did not alter cell viability (Suppl. Fig. 2C).

Lovastatin reverts CSC and invasiveness signatures in mice bearing breast tumors

GSEA revealed that gene sets from a CSR signature (Fig. 6A) and a mammary progenitor cell signature (Fig. 6B) were enriched in mammary tumors of mice that had been treated with vehicle, indicating that *in vivo*, lovastatin downmodulates key genes that are upregulated in the stem/progenitor population of cancer cells. We also queried the dataset with a hallmark set of genes that are upregulated in the EMT (Fig. 6C) and in invasive breast cancer cells (Fig. 6D), given that induction of the EMT promotes the acquisition of CSC features in breast cancer cells [50]. Lovastatin also downregulated these gene sets, suggesting that it shrinks the population with an invasive phenotype and providing indirect evidence of a reduction in the CSC pool.

Finally, the 250 genes with highest differential expression between tumors of lovastatin-treated and vehicle-treated mice were analyzed with regard to enrichment in putative targets of transcription factors (Suppl. Fig. 3). We found that such subset of genes was significantly enriched in targets of transcription factors that control the pluripotency of stem cells or participate in the differentiation of hematopoietic stem cells.

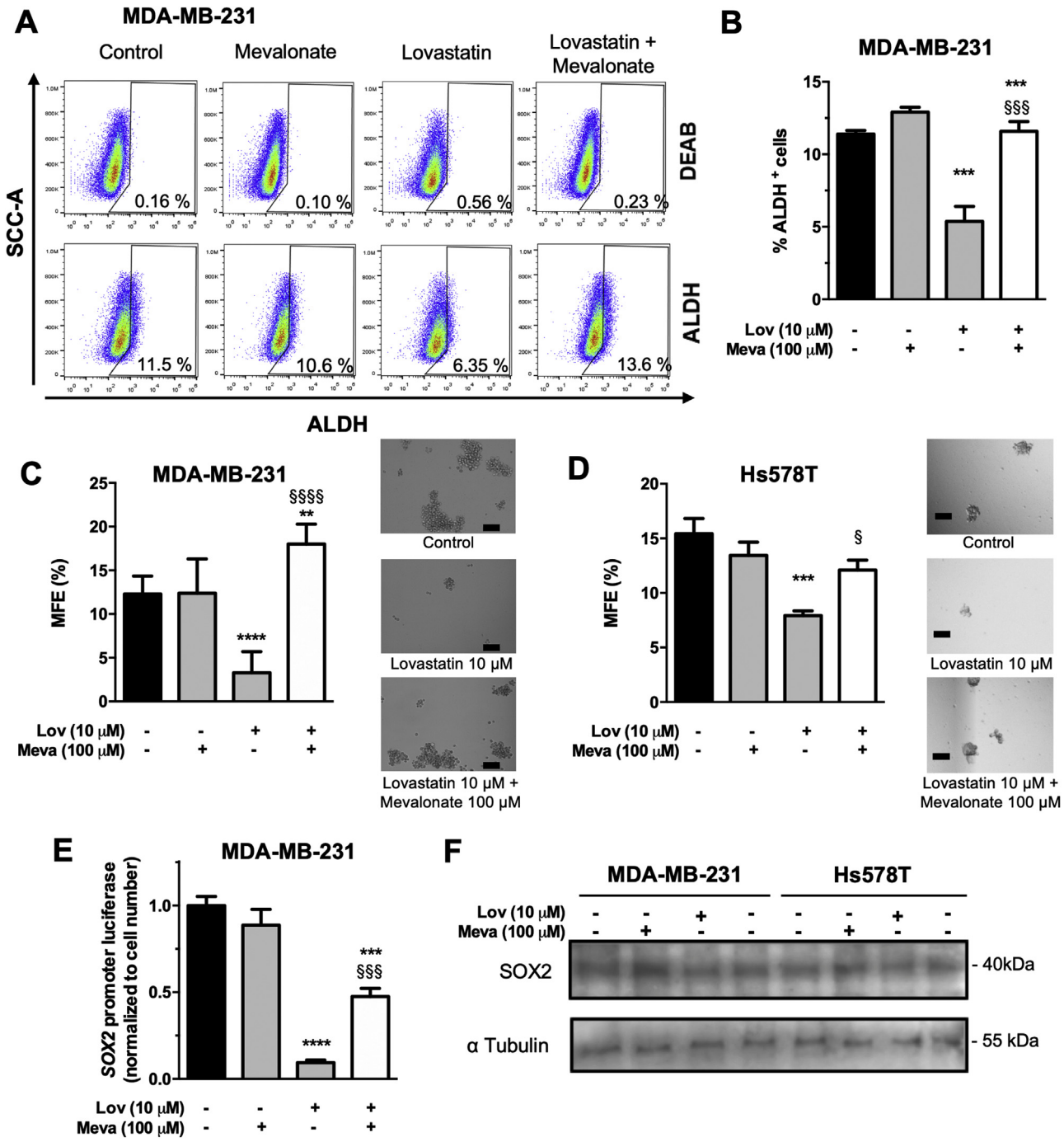

Fig. 5. Effects of mevalonate on lovastatin-induced effects. A) Representative dot plots quantifying the ALDH$^+$ fraction in MDA-MB-231 cells treated with lovastatin (Lov; 10 μM) and/or mevalonate (Meva; 100 μM). B) Quantification of the fraction of ALDH$^+$ cells. Graphs show mean ± SEM from 3 independent experiments. C, D) Mammosphere formation in MDA-MB-231 (C) and Hs578T (D) cells exposed to lovastatin and/or mevalonate for 24 h. Graphs show the mean ± SEM of a representative experiment performed in octuplicate. Representative pictures are shown; bar = 100 μm. E) Transactivation of *SOX2* promoter in MDA-MB-231 cells, assessed by luciferase reporter assay. Values are mean ± SEM of 3 independent experiments. Statistical significance was determined by Tukey's multiple comparisons test against the vehicle control; $p < 0.05$ (*), < 0.01 (**), < 0.001 (***), < 0.0001 (****), and against lovastatin; $p < 0.05$ (§), < 0.001 (§§§), < 0.0001 (§§§§). F) Representative western blot evaluating the expression of SOX2 and α-tubulin in MDA-MB-231 and Hs578T cells exposed to lovastatin and/or mevalonate.

Discussion

The CMap platform allows one to select drugs *in silico*, based on their transcriptional effects on multiple cell lines [24]. Thus, CMap analysis generates hypotheses on the drugs that can revert a particular signature, independent of the cellular context [51,52]. Thus, we aimed to pinpoint drugs that could be repurposed as BCSC-targeting drugs using CMap. Our analysis with a BCSC consensus signature [12] identified 6 candidate drugs with various mechanisms of action. The drugs were structurally dissimilar and induced unrelated global transcriptional profiles, eliminating the possibility that the negative associations with the BCSC signature that were revealed by CMap were elicited through a common mechanism.

Biological evaluation of 5 of the drugs was performed in MDA-MB-231 cells that stably expressed luciferase under control of the

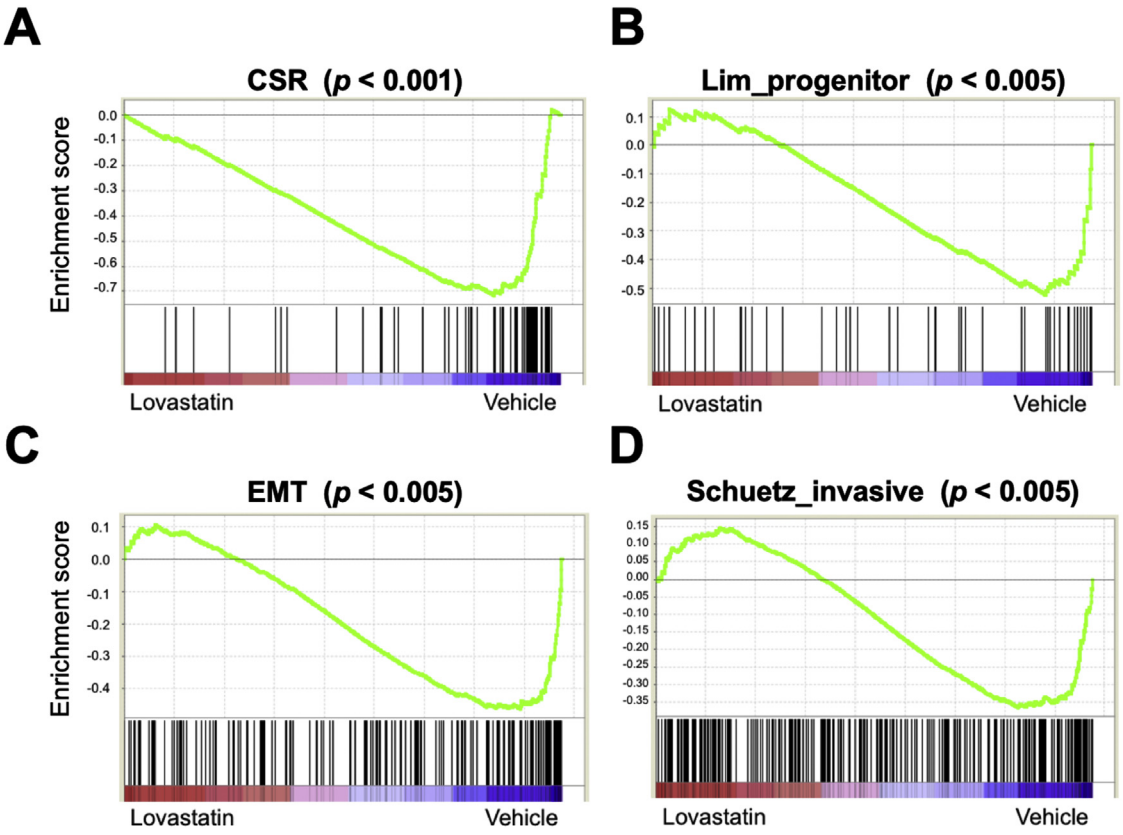

Fig. 6. Enrichment analysis of mammary tumors in mice treated with lovastatin. A–D) Enrichment plots from GSEA. The plots show running enrichment scores (y axis) and positions (black lines) of members of the upregulated gene sets for the CSR (A), luminal progenitors (B), EMT (C), and invasiveness (D).

SOX2 or *OCT4* promoter. Lovastatin and fasudil reduced *SOX2* promotor transactivation, but none of the drugs affected activation of the *OCT4* promoter. SOX2 expression correlates significantly with larger tumors and the presence of lymph node metastases in BC patients [53], and its silencing decreases mammosphere formation *in vitro* and tumorigenicity in animal models [43].

Lovastatin reduced cell viability in adherent cultures of MDA-MB-231 breast cancer cells. Our results are consistent with previous reports that lovastatin induces cell death [54,55] and inhibits the proliferation [56,57] of multiple breast cancer cell lines, including MDA-MB-231.

To validate the CSC-targeting effects of lovastatin, we treated cells for 24 h and analyzed changes in the ALDH$^+$ population, SOX2 expression, and mammosphere formation in drug-free cultures. Lovastatin lowered the ALDH$^+$ fraction, reduced SOX2 protein levels, and irreversibly decreased the number of mammosphere-initiating cells in 2 triple-negative breast cancer cell lines. High ALDH activity marks the BCSC population and correlates with chemoresistance, self-renewal of tumor CSCs, and a poor prognosis in BC patients [46,58], whereas the efficiency of mammosphere formation is a surrogate measure of CSC content [32,59–61]. These effects of lovastatin support the hypothesis that it reduces the CSC pool. Accordingly, previous studies have shown that statins reduce the CSC pool in models of breast [29,30] and other types of cancer [62–64]. Whether BCSC are more sensitive to lovastatin than other subpopulations of breast cancer cells, remains to be determined.

The computational predictions that were generated by CMap do not provide information on whether the transcriptional changes were caused by on-target or off-target effects. Thus, we examined the function of the canonical target of lovastatin in its BCSC-targeting effects. The addition of mevalonate is sufficient to abolish the effects of the inhibition of HMGCR [65]. For example, mevalonate reverses the effects of lovastatin on cell viability [54] and G1 arrest [56]. Supplementation of mevalonate to MDA-MB-231 or Hs578T cells reverted the phenotypic (ALDH$^+$), functional (mammosphere formation), and transcriptional (SOX2) changes that were induced by lovastatin, indicating that its CSC-targeting effects are, at least in part, attributed to the inhibition of HMGCR. Consistent with these findings, previous studies have shown that the effects of statins on the CSC subpopulation are associated with inhibition of the mevalonate pathway [62], which is particularly active on basal BCSCs [30]. However, we cannot disregard the participation of other mechanisms in these effects. For example, a recent study has demonstrated that lovastatin-induced COX-2 expression and the subsequent COX-2-dependent activation of PPARγ cause cytotoxicity in lung cancer cells [66].

Although our *in vitro* results demonstrated CSC-targeting effects of lovastatin, our experiments were designed to use similar concentrations of the drug as in the CMap analysis (10 μM) and in previous reports. Such concentrations are 100- to 1000-fold higher than in plasma of subjects who consume therapeutic doses of lovastatin [67,68], constituting one limitations of the study.

In order to analyze the *in vivo* effects of lovastatin, we studied the transcriptional changes that were induced in mice treated with the drug at a dose (10 mg/kg) that effectively reduces plasma cholesterol [69]. We detected reversions of the gene signatures that define stem/progenitor and invasive cancer cells in mammary tumors of mice that were treated with lovastatin. Lovastatin suppress the expression of a cluster of genes governing EMT, invasion, stemness and apoptosis, including proteins of the Hippo, Notch, Wnt, and HIF pathways [31,55]. Similarly, the administration of atorvastatin to breast cancer patients induces changes in the expression of multiple genes that participate in proliferation

and apoptosis, which may be dependent on changes on the activation of the transcription factors CREB1, ATF, OCT, and SRF [70]. However, the effects of statins on the activation of transcription factors that govern pluripotency are currently unknown. Together, these results validate our *in silico-in vitro* selection, and suggest that lovastatin reduces the stem/progenitor population *in vivo*, warranting further examination.

Conclusion

We have found that lovastatin targets BCSCs by transcriptome-based analysis, combined with *in vitro* evaluations and *in vivo* validation. These effects likely to be caused by the inhibition of HMGCR and thus might be elicited by other statins. Determining the precise mechanisms that are involved in the effects of lovastatin on breast cancer cell stemness might encourage its use as an adjuvant therapeutic strategy for breast tumors.

Conflict of interests

There are no conflicts of interest that are associated with this manuscript.

Funding

This work was supported by PAPIIT UNAMIN228616, CONACYT-INFR-2014-01-225313 (M.A.V-V.), and UDIMEB (S.M.P-T.). L.X.V-B. is recipient of a graduate scholarship from CONACYT (294303).

Author contributions

Luz X. Vásquez-Bochm: Data curation, Formal analysis, Investigation, Visualization, Writing - original draft. Mireya Velázquez-Paniagua: Investigation, Formal analysis, Methodology, Visualization. Sandra S. Castro-Vázquez: Data curation, Formal analysis, Investigation. Sandra L. Guerrero-Rodríguez: Data curation, Formal analysis, Investigation, Visualization. Abimael Mondragon-Peralta: Investigation, Visualization, Formal analysis. Marisol De La Fuente-Granada: Investigation, Visualization, Formal analysis. Sonia M. Pérez-Tapia: Conceptualization, Supervision, Funding acquisition. Aliesha González-Arenas: Conceptualization, Supervision, Funding acquisition, Writing - review and editing. Marco A. Velasco-Velázquez: Conceptualization, Data curation, Formal analysis, Supervision, Funding acquisition, Writing - review and editing.

Acknowledgments

We thank doctors Diana Casique-Aguirre and Angel J. Ruiz Moreno for technical assistance, Mrs. Josefina Bolado, Head of the Scientific Paper Translation Department from División de Investigación at Facultad de Medicina UNAM, for language editing, and Andi Espinoza, Departamento de Farmacología at Facultad de Medicina UNAM, for graphics enhancing.

Appendix A. Supplementary data

Supplementary material related to this article can be found, in the online version, at doi:https://doi.org/10.1016/j.pharep.2019.02.011.

References

[1] McGuire S. World Cancer Report 2014. Geneva, Switzerland: World Health Organization, International Agency For Research on Cancer. WHO Press; 2015 Adv Nutr. 2016;7(2):418-9.
[2] Tao Z, Shi A, Lu C, Song T, Zhang Z, Zhao J. Breast Cancer: epidemiology and etiology. Cell Biochem Biophys 2015;72(2):333–8.
[3] Ahmad A. Pathways to breast cancer recurrence. ISRN Oncol 2013;2013:290568.
[4] Al-Hajj M, Wicha MS, Benito-Hernandez A, Morrison SJ, Clarke MF. Prospective identification of tumorigenic breast cancer cells. Proc Natl Acad Sci U S A 2003;100(7):3983–8.
[5] Seymour T, Twigger AJ, Kakulas F. Pluripotency genes and their functions in the normal and aberrant breast and brain. Int J Mol Sci 2015;16(11):27288–301.
[6] Velasco-Velazquez MA, Popov VM, Lisanti MP, Pestell RG. The role of breast cancer stem cells in metastasis and therapeutic implications. Am J Pathol 2011;179(1):2–11.
[7] Luo M, Clouthier SG, Deol Y, Liu S, Nagrath S, Azizi E, et al. Breast cancer stem cells: current advances and clinical implications. Methods Mol Biol 2015;1293:1–49.
[8] Li X, Lewis MT, Huang J, Gutierrez C, Osborne CK, Wu MF, et al. Intrinsic resistance of tumorigenic breast cancer cells to chemotherapy. J Natl Cancer Inst 2008;100(9):672–9.
[9] Balic M, Lin H, Young L, Hawes D, Giuliano A, McNamara G, et al. Most early disseminated cancer cells detected in bone marrow of breast cancer patients have a putative breast cancer stem cell phenotype. Clin Cancer Res 2006;12(19):5615–21.
[10] Jiao X, Velasco-Velazquez MA, Wang M, Li Z, Rui H, Peck AR, et al. CCR5 governs DNA damage repair and breast Cancer stem cell expansion. Cancer Res 2018;78(7):1657–71.
[11] Baccelli I, Schneeweiss A, Riethdorf S, Stenzinger A, Schillert A, Vogel V, et al. Identification of a population of blood circulating tumor cells from breast cancer patients that initiates metastasis in a xenograft assay. Nat Biotechnol 2013;31(6):539–44.
[12] Gupta PB, Onder TT, Jiang G, Tao K, Kuperwasser C, Weinberg RA, et al. Identification of selective inhibitors of cancer stem cells by high-throughput screening. Cell 2009;138(4):645–59.
[13] Velasco-Velazquez MA, Homsi N, De La Fuente M, Pestell RG. Breast cancer stem cells. Int J Biochem Cell Biol 2012;44(4):573–7.
[14] Wurth R, Thellung S, Bajetto A, Mazzanti M, Florio T, Barbieri F. Drug-repositioning opportunities for cancer therapy: novel molecular targets for known compounds. Drug Discov Today 2016;21(1):190–9.
[15] Cavalla D. Therapeutic switching: a new strategic approach to enhance R&D productivity. IDrugs 2005;8(11):914–8.
[16] Pritchard JE, O'Mara TA, Glubb DM. Enhancing the promise of drug repositioning through genetics. Front Pharmacol 2017;8:896.
[17] Lussier YA, Chen JL. The emergence of genome-based drug repositioning. Sci Transl Med 2011;3(96)96ps35.
[18] Sirota M, Dudley JT, Kim J, Chiang AP, Morgan AA, Sweet-Cordero A, et al. Discovery and preclinical validation of drug indications using compendia of public gene expression data. Sci Transl Med 2011;3(96)96ra77.
[19] Verbist B, Klambauer G, Vervoort L, Talloen W, Consortium Q, Shkedy Z, et al. Using transcriptomics to guide lead optimization in drug discovery projects: lessons learned from the QSTAR project. Drug Discov Today 2015;20(5):505–13.
[20] Iorio F, Rittman T, Ge H, Menden M, Saez-Rodriguez J. Transcriptional data: a new gateway to drug repositioning? Drug Discov Today 2013;18(7-8):350–7.
[21] Iorio F, Bosotti R, Scacheri E, Belcastro V, Mithbaokar P, Ferriero R, et al. Discovery of drug mode of action and drug repositioning from transcriptional responses. Proc Natl Acad Sci U S A 2010;107(33):14621–6.
[22] de Anda-Jauregui G, Guo K, McGregor BA, Hur J. Exploration of the anti-inflammatory drug space through network pharmacology: applications for drug repurposing. Front Physiol 2018;9:151.
[23] Mirza N, Sills GJ, Pirmohamed M, Marson AG. Identifying new antiepileptic drugs through genomics-based drug repurposing. Hum Mol Genet 2017;26(3):527–37.
[24] Lamb J, Crawford ED, Peck D, Modell JW, Blat IC, Wrobel MJ, et al. The Connectivity Map: using gene-expression signatures to connect small molecules, genes, and disease. Science 2006;313(5795):1929–35.
[25] Qu XA, Rajpal DK. Applications of Connectivity Map in drug discovery and development. Drug Discov Today 2012;17(23-24) 1289-98.
[26] Manzotti G, Parenti S, Ferrari-Amorotti G, Soliera AR, Cattelani S, Montanari M, et al. Monocyte-macrophage differentiation of acute myeloid leukemia cell lines by small molecules identified through interrogation of the Connectivity Map database. Cell Cycle 2015;14(16):2578–89.
[27] Zhan SJ, Liu B, Linghu H. Identifying genes as potential prognostic indicators in patients with serous ovarian cancer resistant to carboplatin using integrated bioinformatics analysis. Oncol Rep 2018;39(6):2653–63.
[28] Siavelis JC, Bourdakou MM, Athanasiadis EI, Spyrou GM, Nikita KS. Bioinformatics methods in drug repurposing for Alzheimer's disease. Brief Bioinform 2016;17(2):322–35.
[29] Fiorillo M, Peiris-Pages M, Sanchez-Alvarez R, Bartella L, Di Donna L, Dolce V, et al. Bergamot natural products eradicate cancer stem cells (CSCs) by targeting mevalonate, Rho-GDI-signalling and mitochondrial metabolism. Biochim Biophys Acta 2018;1859(9):984–96.
[30] Ginestier C, Monville F, Wicinski J, Cabaud O, Cervera N, Josselin E, et al. Mevalonate metabolism regulates Basal breast cancer stem cells and is a potential therapeutic target. Stem Cells 2012;30(7):1327–37.
[31] Koohestanimobarhan S, Salami S, Imeni V, Mohammadi Z, Bayat O. Lipophilic statins antagonistically alter the major epithelial-to-mesenchymal transition

signaling pathways in breast cancer stem-like cells via inhibition of the mevalonate pathway. J Cell Biochem 2018.
[32] Dontu G, Abdallah WM, Foley JM, Jackson KW, Clarke MF, Kawamura MJ, et al. In vitro propagation and transcriptional profiling of human mammary stem/progenitor cells. Genes Dev 2003;17(10):1253–70.
[33] Shipitsin M, Campbell LL, Argani P, Weremowicz S, Bloushtain-Qimron N, Yao J, et al. Molecular definition of breast tumor heterogeneity. Cancer Cell 2007;11(3):259–73.
[34] Wu K, Jiao X, Li Z, Katiyar S, Casimiro MC, Yang W, et al. Cell fate determination factor Dachshund reprograms breast cancer stem cell function. J Biol Chem 2011;286(3):2132–42.
[35] Schneider CA, Rasband WS, Eliceiri KW. NIH Image to ImageJ: 25 years of image analysis. Nat Methods 2012;9(7):671–5.
[36] Mira E, Carmona-Rodriguez L, Tardaguila M, Azcoitia I, Gonzalez-Martin A, Almonacid L, et al. A lovastatin-elicited genetic program inhibits M2 macrophage polarization and enhances T cell infiltration into spontaneous mouse mammary tumors. Oncotarget 2013;4(12):2288–301.
[37] Subramanian A, Tamayo P, Mootha VK, Mukherjee S, Ebert BL, Gillette MA, et al. Gene set enrichment analysis: a knowledge-based approach for interpreting genome-wide expression profiles. Proc Natl Acad Sci U S A 2005;102(43):15545–50.
[38] Shats I, Gatza ML, Chang JT, Mori S, Wang J, Rich J, et al. Using a stem cell-based signature to guide therapeutic selection in cancer. Cancer Res 2011;71(5):1772–80.
[39] Lim E, Wu D, Pal B, Bouras T, Asselin-Labat ML, Vaillant F, et al. Transcriptome analyses of mouse and human mammary cell subpopulations reveal multiple conserved genes and pathways. Breast Cancer Res 2010;12(2):R21.
[40] Liberzon A, Birger C, Thorvaldsdottir H, Ghandi M, Mesirov JP, Tamayo P. The Molecular Signatures Database (MSigDB) hallmark gene set collection. Cell Syst 2015;1(6):417–25.
[41] Schuetz CS, Bonin M, Clare SE, Nieselt K, Sotlar K, Walter M, et al. Progression-specific genes identified by expression profiling of matched ductal carcinomas in situ and invasive breast tumors, combining laser capture microdissection and oligonucleotide microarray analysis. Cancer Res 2006;66(10):5278–86.
[42] Lachmann A, Xu H, Krishnan J, Berger SI, Mazloom AR, Ma'ayan A. ChEA: transcription factor regulation inferred from integrating genome-wide ChIP-X experiments. Bioinformatics 2010;26(19):2438–44.
[43] Leis O, Eguiara A, Lopez-Arribillaga E, Alberdi MJ, Hernandez-Garcia S, Elorriaga K, et al. Sox2 expression in breast tumours and activation in breast cancer stem cells. Oncogene 2012;31(11):1354–65.
[44] Nishi M, Sakai Y, Akutsu H, Nagashima Y, Quinn G, Masui S, et al. Induction of cells with cancer stem cell properties from nontumorigenic human mammary epithelial cells by defined reprogramming factors. Oncogene 2014;33(5):643–52.
[45] Tang B, Raviv A, Esposito D, Flanders KC, Daniel C, Nghiem BT, et al. A flexible reporter system for direct observation and isolation of cancer stem cells. Stem Cell Reports 2015;4(1):155–69.
[46] Ginestier C, Hur MH, Charafe-Jauffret E, Monville F, Dutcher J, Brown M, et al. ALDH1 is a marker of normal and malignant human mammary stem cells and a predictor of poor clinical outcome. Cell Stem Cell 2007;1(5):555–67.
[47] Croker AK, Goodale D, Chu J, Postenka C, Hedley BD, Hess DA, et al. High aldehyde dehydrogenase and expression of cancer stem cell markers selects for breast cancer cells with enhanced malignant and metastatic ability. J Cell Mol Med 2009;13(8B):2236–52.
[48] Croker AK, Allan AL. Inhibition of aldehyde dehydrogenase (ALDH) activity reduces chemotherapy and radiation resistance of stem-like ALDHhiCD44(+) human breast cancer cells. Breast Cancer Res Treat 2012;133(1):75–87.
[49] Goldstein JL, Brown MS. Regulation of the mevalonate pathway. Nature 1990;343(6257):425–30.
[50] Mani SA, Guo W, Liao MJ, Eaton EN, Ayyanan A, Zhou AY, et al. The epithelial-mesenchymal transition generates cells with properties of stem cells. Cell 2008;133(4):704–15.
[51] Gao L, Zhao G, Fang JS, Yuan TY, Liu AL, Du GH. Discovery of the neuroprotective effects of alvespimycin by computational prioritization of potential anti-Parkinson agents. FEBS J 2014;281(4):1110–22.
[52] Beck A, Eberherr C, Hagemann M, Cairo S, Haberle B, Vokuhl C, et al. Connectivity map identifies HDAC inhibition as a treatment option of high-risk hepatoblastoma. Cancer Biol Ther 2016;17(11):1168–76.
[53] Zheng Y, Qin B, Li F, Xu S, Wang S, Li L. Clinicopathological significance of Sox2 expression in patients with breast cancer: a meta-analysis. Int J Clin Exp Med 2015;8(12):22382–92.
[54] Siddiqui RA, Harvey KA, Xu Z, Natarajan SK, Davisson VJ. Characterization of lovastatin-docosahexaenoate anticancer properties against breast cancer cells. Bioorg Med Chem 2014;22(6):1899–908.
[55] Yang T, Yao H, He G, Song L, Liu N, Wang Y, et al. Effects of lovastatin on MDA-MB-231 breast Cancer cells: an antibody microarray analysis. J Cancer 2016;7(2):192–9.
[56] Rao S, Porter DC, Chen X, Herliczek T, Lowe M, Keyomarsi K. Lovastatin-mediated G1 arrest is through inhibition of the proteasome, independent of hydroxymethyl glutaryl-CoA reductase. Proc Natl Acad Sci U S A 1999;96(14):7797–802.
[57] Campbell MJ, Esserman LJ, Zhou Y, Shoemaker M, Lobo M, Borman E, et al. Breast cancer growth prevention by statins. Cancer Res 2006;66(17):8707–14.
[58] Magni M, Shammah S, Schiro R, Mellado W, Dalla-Favera R, Gianni AM. Induction of cyclophosphamide-resistance by aldehyde-dehydrogenase gene transfer. Blood 1996;87(3):1097–103.
[59] Liao MJ, Zhang CC, Zhou B, Zimonjic DB, Mani SA, Kaba M, et al. Enrichment of a population of mammary gland cells that form mammospheres and have in vivo repopulating activity. Cancer Res 2007;67(17):8131–8.
[60] Ponti D, Costa A, Zaffaroni N, Pratesi G, Petrangolini G, Coradini D, et al. Isolation and in vitro propagation of tumorigenic breast cancer cells with stem/progenitor cell properties. Cancer Res 2005;65(13):5506–11.
[61] Lombardo Y, de Giorgio A, Coombes CR, Stebbing J, Castellano L. Mammosphere formation assay from human breast cancer tissues and cell lines. J Vis Exp 2015;97:.
[62] Brandi J, Dando I, Pozza ED, Biondani G, Jenkins R, Elliott V, et al. Proteomic analysis of pancreatic cancer stem cells: functional role of fatty acid synthesis and mevalonate pathways. J Proteomics 2017;150:310–22.
[63] Peng Y, He G, Tang D, Xiong L, Wen Y, Miao X, et al. Lovastatin inhibits Cancer stem cells and sensitizes to Chemo- and photodynamic therapy in nasopharyngeal carcinoma. J Cancer 2017;8(9):1655–64.
[64] Kato S, Liberona MF, Cerda-Infante J, Sanchez M, Henriquez J, Bizama C, et al. Simvastatin interferes with cancer' stem-cell' plasticity reducing metastasis in ovarian cancer. Endocr Relat Cancer 2018;25(10):821–36.
[65] Alonso DF, Farina HG, Skilton G, Gabri MR, De Lorenzo MS, Gomez DE. Reduction of mouse mammary tumor formation and metastasis by lovastatin, an inhibitor of the mevalonate pathway of cholesterol synthesis. Breast Cancer Res Treat 1998;50(1):83–93.
[66] Walther U, Emmrich K, Ramer R, Mittag N, Hinz B. Lovastatin lactone elicits human lung cancer cell apoptosis via a COX-2/PPARgamma-dependent pathway. Oncotarget 2016;7(9):10345–62.
[67] Neuvonen PJ, Jalava KM. Itraconazole drastically increases plasma concentrations of lovastatin and lovastatin acid. Clin Pharmacol Ther 1996;60(1):54–61.
[68] Kyrklund C, Backman JT, Kivisto KT, Neuvonen M, Laitila J, Neuvonen PJ. Plasma concentrations of active lovastatin acid are markedly increased by gemfibrozil but not by bezafibrate. Clin Pharmacol Ther 2001;69(5):340–5.
[69] van de Steeg E, Kleemann R, Jansen HT, van Duyvenvoorde W, Offerman EH, Wortelboer HM, et al. Combined analysis of pharmacokinetic and efficacy data of preclinical studies with statins markedly improves translation of drug efficacy to human trials. J Pharmacol Exp Ther 2013;347(3):635–44.
[70] Bjarnadottir O, Kimbung S, Johansson I, Veerla S, Jonsson M, Bendahl PO, et al. Global transcriptional changes following statin treatment in breast Cancer. Clin Cancer Res 2015;21(15):3402–11.